forests

MDPI

Article

Identifying Even- and Uneven-Aged Forest Stands Using Low-Resolution Nationwide Lidar Data

Anže Martin Pintar [1,2,*] and Mitja Skudnik [1,2]

[1] Slovenian Forestry Institute, Večna pot 2, 1000 Ljubljana, Slovenia; mitja.skudnik@gozdis.si
[2] Biotechnical Faculty, University of Ljubljana, Jamnikarjeva 101, 1000 Ljubljana, Slovenia
* Correspondence: anzemartin.pintar@gozdis.si

Abstract: In uneven-aged forests, trees of different diameters, heights, and ages are located in a small area, which is due to the felling of individual trees or groups of trees, as well as small-scale natural disturbances. In this article, we present an objective method for classifying forest stands into even- and uneven-aged stands based on freely available low-resolution (with an average recording density of 5 points/m^2) national lidar data. The canopy closure, dominant height, and canopy height diversity from the canopy height model and the voxels derived from lidar data were used to classify the forest stands. Both approaches for determining forest structural diversity (canopy height diversity—CHD_{CHM} and CHD_V) yielded similar results, namely two clusters of even- and uneven-aged stands, although the differences in vertical diversity between even- and uneven-aged stands were greater when using CHM. The first analysis, using CHM for the *CHD* assessment, estimated the uneven-aged forest area as 49.3%, whereas the second analysis using voxels estimated it as 34.3%. We concluded that in areas with low laser scanner density, CHM analysis is a more appropriate method for assessing forest stand height heterogeneity. The advantage of detecting uneven-aged structures with voxels is that we were able to detect shade-tolerant species of varying age classes beneath a dense canopy of mature, dominant trees. The CHD_{CHM} values were estimated to be 1.83 and 1.86 for uneven-aged forests, whereas they were 1.57 and 1.58 for mature even-aged forests. The CHD_V values were estimated as 1.50 and 1.62 for uneven-aged forests, while they were 1.33 and 1.48 for mature even-aged forests. The classification of stands based on lidar data was validated with data from measurements on permanent sample plots. Statistically significantly lower average values of the homogeneity index and higher values of the Shannon–Wiener index from field measurements confirm the success of the classification of stands based on lidar data as uneven-aged forests.

Keywords: uneven-aged forest; lidar data; canopy height model; voxels; canopy height diversity

Citation: Pintar, A.M.; Skudnik, M. Identifying Even- and Uneven-Aged Forest Stands Using Low-Resolution Nationwide Lidar Data. *Forests* **2024**, *15*, 1407. https://doi.org/10.3390/f15081407

Academic Editor: Qingsheng Liu

Received: 30 July 2024
Revised: 8 August 2024
Accepted: 9 August 2024
Published: 11 August 2024

1. Introduction

In uneven-aged forests, trees of different diameters, heights, and ages are located in a small area. This structural diversity arises from specific silvicultural treatments involving the selective felling of individual trees or small groups [1], as well as small-scale natural disturbances [2]. In addition to species composition, the diverse structure of forests affects not only biodiversity but also their resilience to abiotic and biotic damage [3], along with forest productivity [4] and other processes in forests such as water balance, the distribution of carbon stocks, nutrient cycling, and light dynamics [5].

In Central Europe, regeneration in natural, unmanaged forests usually occurs in small gaps [6]. A forest with a heterogeneous structure does not have the same regeneration pattern over large areas, and regeneration is concentrated only in a small area of gaps. A mixture of small and large gaps in the forest is a good approach to improving the diversity of forest habitats [6]. Currently, even-aged forests still predominate in Europe [7], and due to the higher resilience of uneven-aged forests to disturbances, calamities, and climate change [8,9], as well as the faster recovery of these forests after disturbances, the

proportion of uneven-aged forests in both Europe and worldwide is expected to increase in the future. This has already led to an increased need for the development and management of uneven-aged mixed forests in recent years, as these forests are considered more resilient to disturbances and have a higher adaptive potential [10].

Slovenia is dominated by uneven-aged forests [11] due to a long tradition of small-scale forest management [12]. The most typical uneven-aged forests in Slovenia are mixed fir–beech–spruce forests on carbonates in the Dinarides and the Alps and mixed fir–spruce forests on silicates, which have been sustainably managed for at least half a century [13–15]. The forests in the wider Pohorje region are also an example of uneven-aged forest structures in spruce–fir forests on silicates [11]. This region was selected for our study due to its representative uneven-aged forest structures, providing an ideal setting to develop and validate our classification method using low-resolution nationwide lidar data.

The structure of uneven-aged forest stands can be described using vertical (e.g., number of tree layers, etc.) and horizontal elements (e.g., the spatial distribution of trees, gaps, etc.), as well as species diversity [16]. The structure of forest stands can be described considering the number of trees, tree species composition, height, and diameter-at-breast-height distribution of the trees [17]. Assessing the vertical and horizontal structures of uneven-aged forest stands is crucial for supporting forest management activities, for instance, for planning silvicultural measures, assessing the suitability of habitats for rare and endangered species [18], and subsequently stratifying forest stands by forest habitat types, as presented by Hladnik and Žižek Kulovec [19] for the case of Slovenia. The vertical forest structure, which is often challenging to quantify objectively, is essential in forest management planning [20]. Currently, indicators used to describe vertical structures frequently rely on visual estimation, which can be highly subjective and vary significantly between different observers.

Additionally, using detailed data from field measurements to assess the horizontal and vertical structures of uneven-aged forest stands is labor-intensive and costly due to the extensive fieldwork required, especially when many stands need to be surveyed over large forest areas, most notably in forests with mixed ownership [21]. Currently, stand maps need to be rapidly updated given the increasingly frequent natural disturbances [22]. Another challenge in field measurement is the objectivity of data collection by individual teams. One of the main advantages of using remote sensing data for forest structure assessment is providing a more rapid and cost-effective approach to obtaining accurate and objective data for larger areas [23].

This study explores the following question: how can freely available national lidar data be used to objectively classify forest stands into even- and uneven-aged categories? We hypothesized that nationwide, low-resolution lidar data can effectively distinguish between even- and uneven-aged forest stand structures. This, in turn, will enable forest managers to identify uneven-aged stands over larger areas more objectively and efficiently. Furthermore, this method can be reapplied as new lidar data become available, offering a more cost-effective, scalable, and up-to-date approach for forest structure assessment compared to traditional field methods.

This study aims to present an objective method for classifying forest stands into even- and uneven-aged stands based on freely available national lidar data [24]. The study findings contribute to more resilient forest management strategies and support the sustainable management of forest resources in Slovenia and beyond.

2. Materials and Methods

2.1. Study Area

The study area encompasses the wider forest area of the Pahernik forest estate (Figure 1), which was selected due to the presence of a diverse forest structure [25–27] and because it is a large forest estate that has undergone more than a century of planned forest management [25] through the development of an uneven-aged forest structure. Additionally, a denser network of permanent sample plots (250 × 250 m) is available, with a

detailed estate plan (2014–2023) prepared by the Slovenian Forest Service based on field measurements [28].

The study area is located in the northeastern part of Slovenia on the Drava–Pohorje mountain range, between the Drava River in the north and the Pohorje mountain ridge in the south, in the northeastern part of Slovenia. Field measurements have already revealed that the area has an uneven-aged forest structure [26]. The predominant tree species is Norway spruce (*Picea abies*), accounting for more than 60% of the growing stock, and more than 10% of the growing stock is silver fir (*Abies alba*) and European beech (*Fagus sylvatica*) [26]. Forests account for 4479 ha of the surveyed area. A forest mask was taken from the survey on the actual use of agricultural and forest land provided by the Ministry of Agriculture, Forestry, and Food [29].

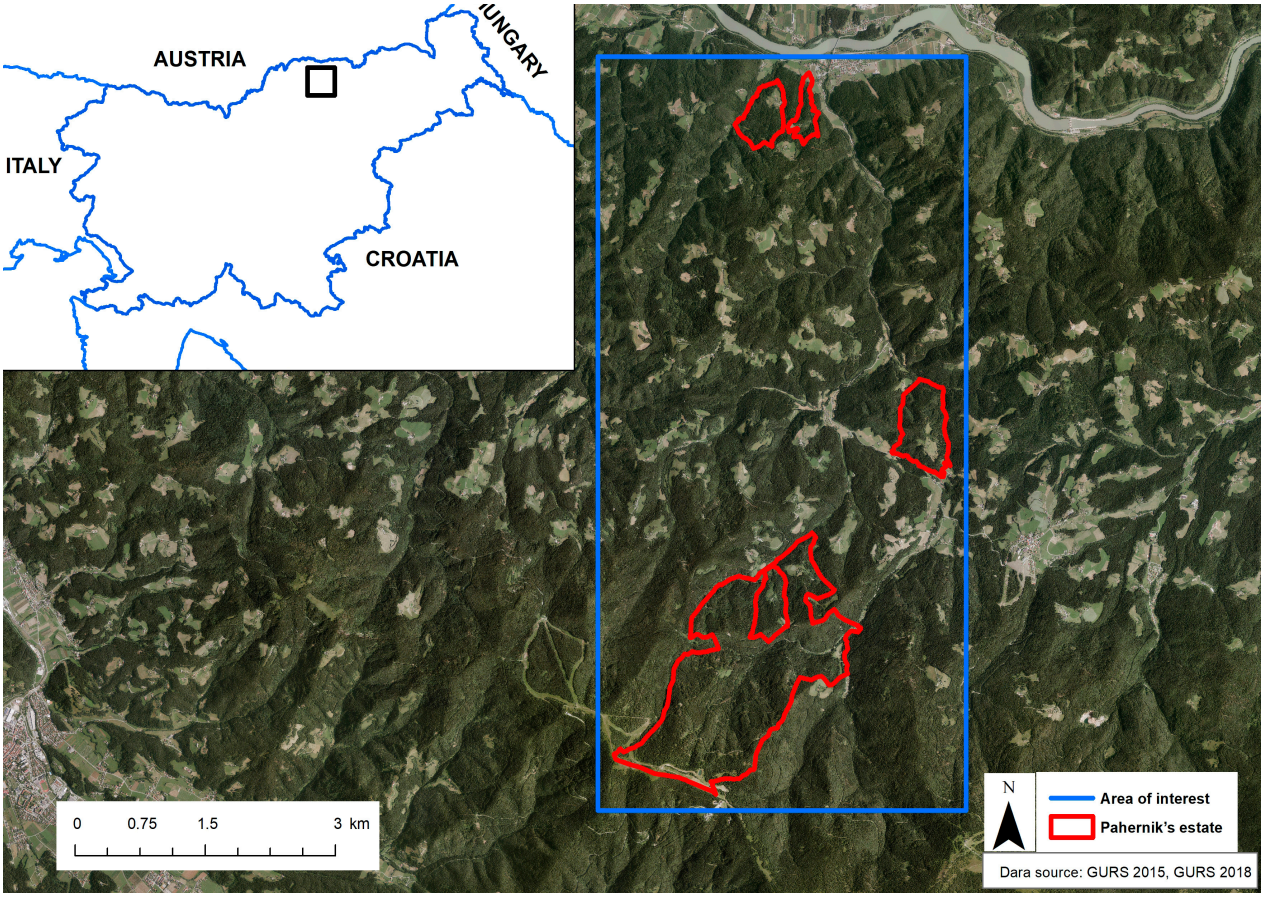

Figure 1. The Pahernik estate and the entire study area.

2.2. Data Preparation

The forest structure was assessed based on freely available national lidar data, which were recorded on tree foliage in 2014 [30]. The laser scanning of Slovenia was carried out with the Eurocopter EC 120B helicopter at flight height from 1200 to 1400 m above the ground. The lidar system consisted of a RIEGL LMS-Q780 laser scanner with a pulse frequency of 400 kHz and a positioning and orientation system (differential GNSS Novatel OEMV-3, INS IGI Aerocontrol Mark II rotation measurement system (E 256 Hz)). The average recording density was 5 points/m^2 with a laser beam diameter or a footprint with a size of 30 cm, a positional accuracy of 30 cm, and an ellipsoidal height accuracy of 15 cm [30].

To determine the vegetation height, we used a canopy height model (CHM) developed by Kobler [31], using a resolution of 1 m. In the studied area, the digital canopy model obtained from the laser scanning data of Slovenia was segmented considering the minimum

segment size of 5000 pixels, proposed by Šprah [32], as optimal for the eastern part of Pohorje, as smaller values indicate significantly smaller groups and clumps and dictate the method of regeneration in the area. Thus, we obtained a raster map of CHM segments that represented forest stands (Figure 2).

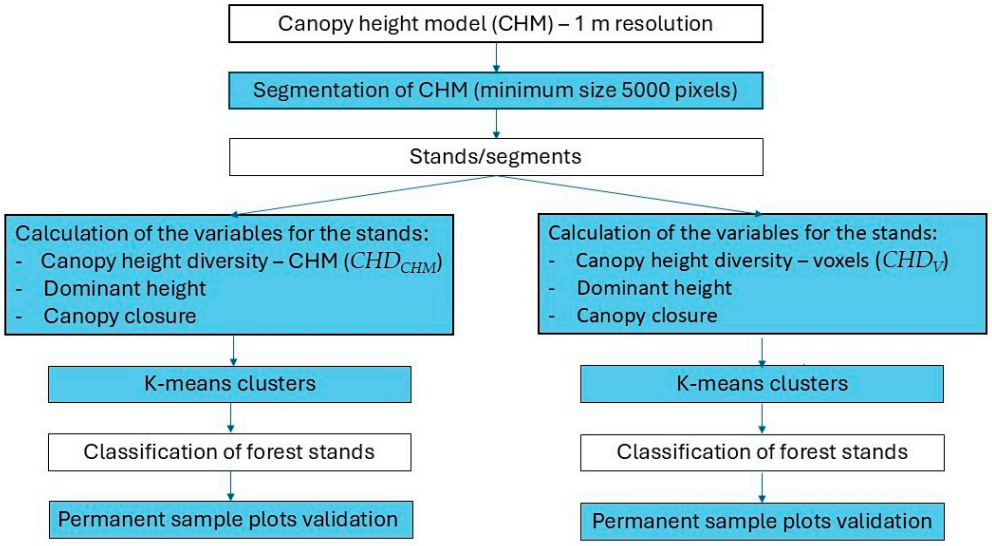

Figure 2. Flowchart for the classification and validation of the forest stands.

In the canopy height model, we searched for local maxima considering circular neighborhood associations with a radius of 3 m, which was chosen based on measurements of tree canopy radii for prevalent species in the area, as presented by Pretzsch, et al. [33]. We then recorded tree height data and thus obtained a digital model of the tree tops or stand canopy. Considering the 100 highest trees per hectare [34], we determined the dominant height of trees for the entire stand or segment (Figure 2). We also calculated the canopy closure for each of the analyzed stands. The canopy closure (Figure 2) is the proportion of the area in the canopy height model with height classes higher than 5 m.

The digital canopy model was classified into 5 m height classes, according to the FAO [35]. This classification system was used by Hladnik, et al. [36] in their study on Slovenian forests and by Šprah [32], whose study investigated the Pohorje region near our study area; in both cases, it proved to be suitable. The first class includes tree heights from 0 to 5 m, and the last class encompasses tree heights above 40 m. For each stand derived from segmentation, we calculated the area of each height class and its proportion. From these data, we then calculated the canopy height diversity (CHD_{CHM}) using Equation (1) (Figure 2). Similar indices for assessing the vertical forest structure have already been proposed [36–39]. The p_i value represents the proportion of the area of each height class in the total area of the forest stand.

$$CHD_{CHM} = -\sum p_i \ln(p_i), \quad (1)$$

Using a resolution of 10 m, we generated raster maps from the lidar point cloud considering the relative frequencies of reflections along 5 m height classes (voxels), as established by Kobler [40]. These maps were then used to create a raster map of canopy height diversity using voxels (CHD_V, Equation (2)) for the entire study area (Figure 2).

$$CHD_V = -\sum p_i \ln(p_i), \quad (2)$$

To classify forests as even- and uneven-aged structures, we investigated the use of CHD_{CHM} and CHD_V. CHM is more intuitive [36] and easier to use in operational practice [41] when studying larger areas, but its disadvantage is that some shade-tolerant trees

cannot be detected when there is a dense canopy of mature dominant trees in stands with low-height diversity visible from above, in contrast to the approach using voxels [42–45].

2.3. Statistical Analysis

2.3.1. Classification of Stands/Segments into Stand Types

Two K-means cluster analyses (Figure 2) were used to classify the stands derived from segmentation. Clustering involves a broad range of techniques for exploring subgroups within a dataset, which requires categorizing similar observations into the same group and dissimilar observations into different groups [46]. We used this analysis because it has proven useful, for example, for the typification of forest edges [36] and tree species according to canopy characteristics [47]. In the first analysis, we used the canopy height diversity derived from the proportions of the individual height classes of the digital canopy model (CHD_{CHM}), the variable dominant height of the stands, and the canopy closure to estimate the vertical diversity of the stands. In the second analysis, we used the canopy height diversity derived from the ratio of the relative frequencies of reflections by height classes (voxels (CHD_V)), and the variables dominant height of the canopy of the stands, and canopy closure. We identified the optimal number of clusters using the elbow method, which minimized the total within-cluster variation [46].

2.3.2. Permanent Sample Plots

In the study area, we analyzed 91 sample plots, with a radius of 12.61 m and an area was 500 m^2, using a systematic sample grid of 250 × 250 m measured in 2013 by the Slovenia Forest Service [28]. The radius of the sample plot was 12.61 m and the area was 500 m^2. We used permanent sample plots from this inventory as the Slovenia Forest Service has a dense sampling network throughout the country, and plots are measured every 10 years. The Slovenia Forest Service is a public institution that oversees forestry planning and management for all Slovenian forests, irrespective of ownership [48]. Every year, 1⁄10 plans are renewed, and a field inventory consisting of permanent sample plots and field descriptions of forest stands is carried out. In this study, trees with a diameter at breast height of 30 cm or more were measured using the entire sample plot. In the inner part of the plot, with a radius of 7.98 m and an area of 200 m^2, trees with a diameter at breast height of 10 cm or more were also measured. Tree height was also measured for all trees included in the canopy of the stand in the sample plot (720 trees). The coordinates of the center of each plot were measured using a handheld GPS receiver. The location of each tree was determined by the distance from the center of the plot and the azimuth, i.e., the angle between north and the location of the tree. The sample plots were then accurately positioned based on the correspondence between the location of the dominant trees determined from the field measurements and the same trees identified on the generated lidar CHM.

Regarding the structural diversity of the forest stands, the Shannon–Wiener index (H') was calculated for each sample plot. *Pi* represents the proportion of basal area per hectare of each tree species or the proportion of basal area per hectare of trees in each diameter class to the total basal area (Equation (3)).

$$H' = -\sum p_i \ln(p_i), \tag{3}$$

For each sample plot, we also calculated the De Camino homogeneity index [49], which has already been used to determine the homogeneity of spruce–fir forests [50]. The homogeneity index is calculated using Equation (4) [49]:

$$CH = \frac{\sum_{i=1}^{n-1} SN\%}{\sum_{i=1}^{n-1} SN\% - SV\%} \tag{4}$$

where $SN\%$ is the sum of percentages of the number of trees up to the ith diameter class, $SV\%$ is the sum of percentages of the volume up to the ith diameter class, and n is the number of diameter classes.

To overlap the remote sensing data with the data measured in the field, we used permanent sample plots that covered at least 80% of each segment considering cases in which the difference between the measured and lidar-estimated dominant height of the corresponding segment was less than 5 m. In this way, plots that were within a small core of other development phases of the stands were excluded from further analysis, as they were too small for independent analysis.

Of the 91 permanent sample plots, 39 were used for further analysis (Figure 2). This reduction in number was mainly due to the diversity of forests throughout the area, which resulted in some sample plots being located at the boundary of the homogenous stands obtained using segmentation.

Spatial analyses were carried out using ArcMap 10.8 [51], and all statistical analyses and graph generations were performed using the R 3.5.2 software [52].

3. Results

3.1. Classification of Stands/Segments into Structural Types

In the first analysis, the CHM was used to estimate the canopy height diversity. Clusters 2 and 4 had the highest average canopy height diversity (Table 1; Figure 3a), thus representing the clusters with the most diverse stands. Cluster 4 had a slightly higher average canopy height, but the two clusters differed in the average dominant height, with Cluster 4 being more than 8 m higher. Clusters 1 and 3 had comparable average dominant heights but lower average canopy height diversity (CHD_{CHM}) (Figure 4). Clusters 5 and 6 were associated with development phases with a lower dominant height. The lowest average dominant height, the lowest canopy closure, and the lowest canopy height diversity were observed in Cluster 5, representing seedlings and stands in regeneration (Figure 5). All variables in this cluster had a maximum coefficient of variation of more than 20% (Table 1, Figure 3). Cluster 6, representing pole stands, had higher average values of the investigated variables than Cluster 5 (Figure 5).

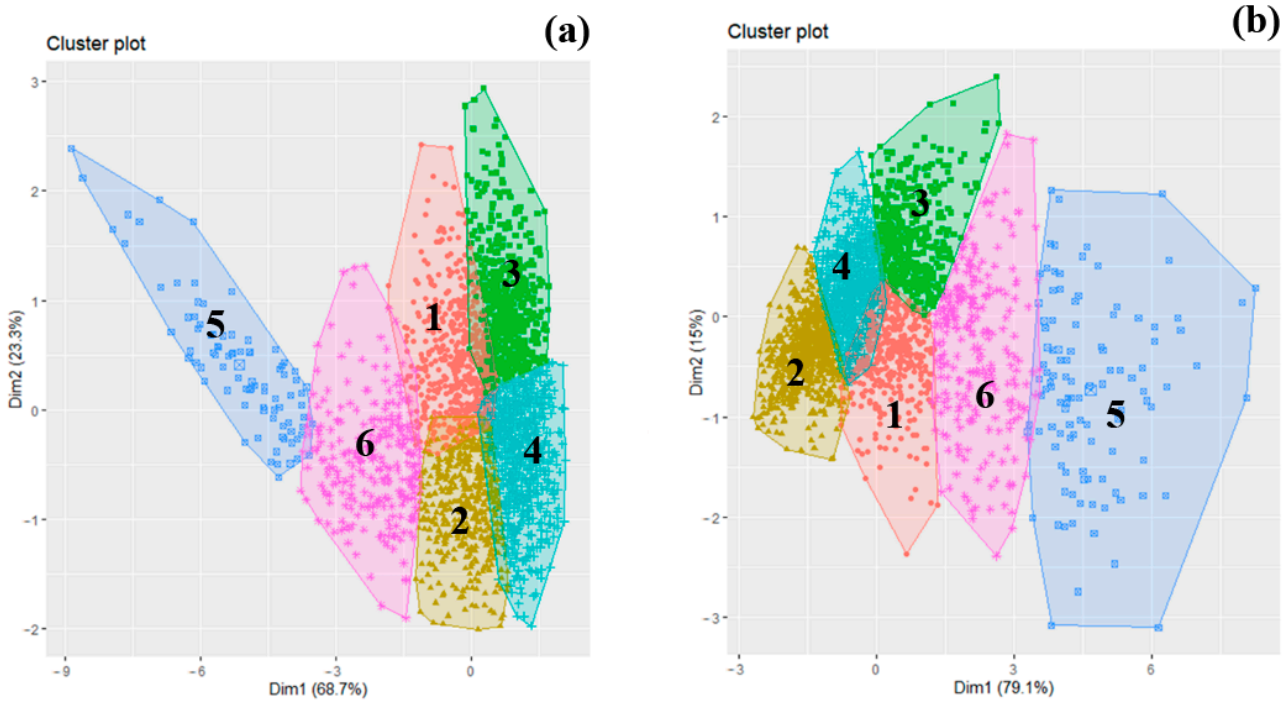

Figure 3. Classification of forest stands in clusters. CHM (**a**) and VOXELS (**b**) were used to assess the canopy height diversity.

Table 1. Area, dominant height, canopy closure, and canopy height diversity using CHM (CHD_{CHM}) by individual classes of stand types.

Cluster	Area (ha)	H_{dom} (m)	SD_1	CV_1 (%)	Canopy Closure	SD_2	CV_2 (%)	CHD_{CHM}	SD_3	CV_3 (%)
1	966.5	26.5	3.1	11.8	0.93	0.04	4.7	1.57	0.11	6.8
2	815.5	26.2	2.8	10.6	0.85	0.06	7.3	1.83	0.09	5.0
3	874.3	36.3	3.1	8.6	0.97	0.02	2.3	1.58	0.11	6.9
4	1395.2	34.3	3.1	9.1	0.93	0.04	4.1	1.86	0.10	5.3
5	123.4	12.4	3.1	24.7	0.37	0.11	28.9	1.10	0.22	20.1
6	304.4	18.8	2.7	14.6	0.68	0.10	14.3	1.55	0.12	7.9

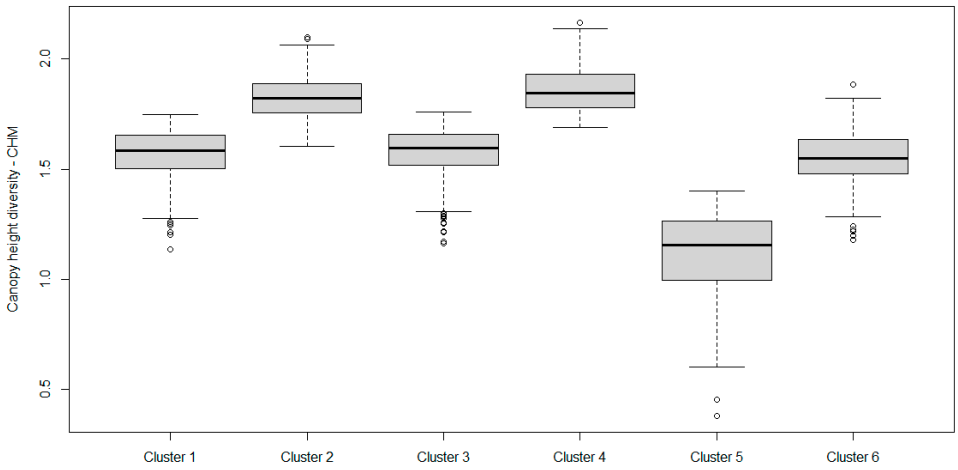

Figure 4. Boxplots for the CHD_{CHM} by individual clusters of stand types.

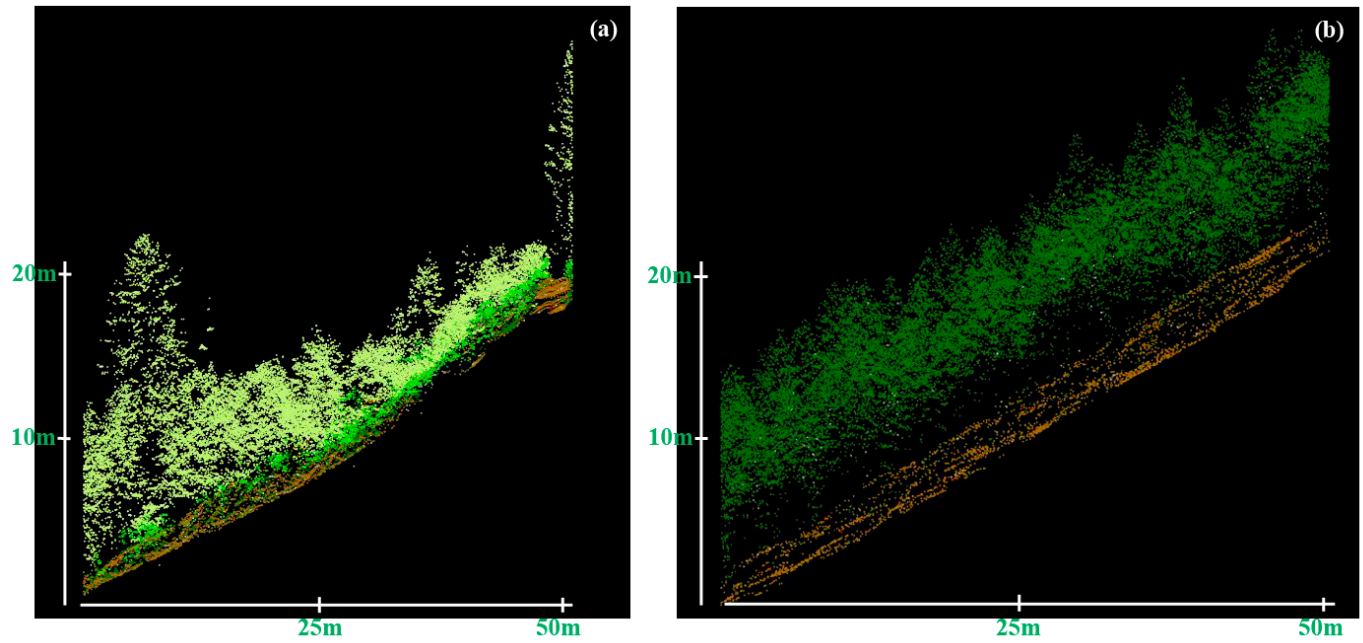

Figure 5. Examples of the cross-section of a lidar point cloud of a stand undergoing regeneration with reservation of standards (Cluster 5 (**a**)) and a pole stand (Cluster 6 (**b**)).

In Clusters 2 and 4, which were classified as uneven-aged stands, the mean standard deviation (SD) for the dominant height within of each stand was higher (5.9 and 4.0 m) than those in Clusters 1 and 3, classified as even-aged stands (2.9 and 2.5 m) (Figure 6). Clusters

5 (7.8 m) and 6 (6.6 m), associated with seedlings and stands undergoing regeneration and pole stands, respectively, had the highest SD values (Figure 6), which can be attributed to the small-scale management practices with reservation of standards.

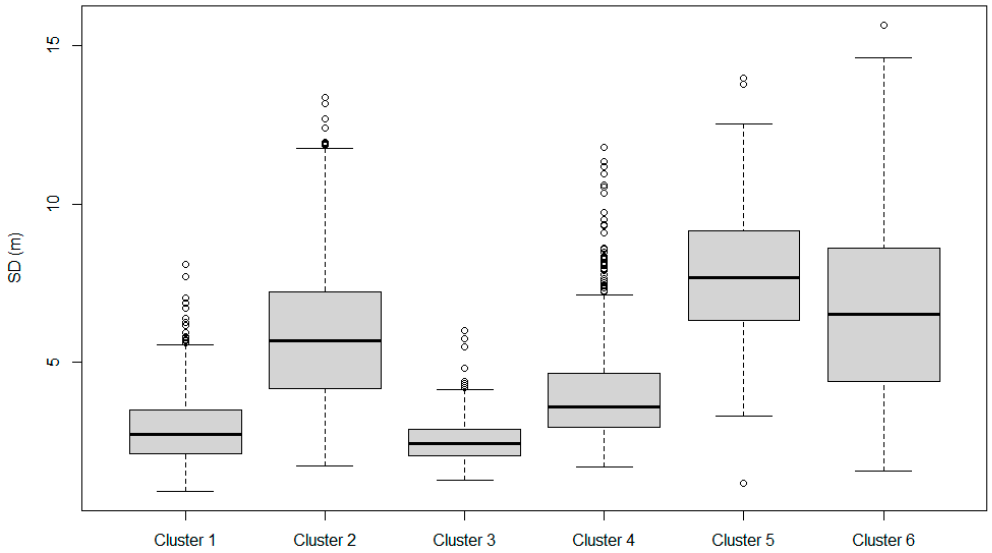

Figure 6. Boxplots for the SD for dominant height for each analyzed stand by individual clusters of stand types.

In the second analysis, we used voxels to estimate the canopy height diversity. Cluster 2 had the highest average value of canopy height diversity (CHD_V) (Table 2; Figures 3, 7 and 8), representing the most uneven-aged stands. The CHD_V was also high for Clusters 1 and 4. Cluster 1 had a lower average dominant height and a lower canopy closure than Cluster 4. Clusters 5 and 6 represented the development stages with a lower dominant height. Cluster 5, representing seedlings and stands in the regeneration phase (Figure 5a) had the lowest average dominant height, the lowest canopy closure, and the lowest CHD_V, as shown in Figure 7. All variables in this cluster had a maximum coefficient of variation higher than 20% (Table 2, Figure 3). Cluster 6, encompassing pole stands, had higher average values for the analyzed variables than Cluster 5. Cluster 3, identified as the cluster with mature even-aged stands, had an average dominant height of 25.4 m.

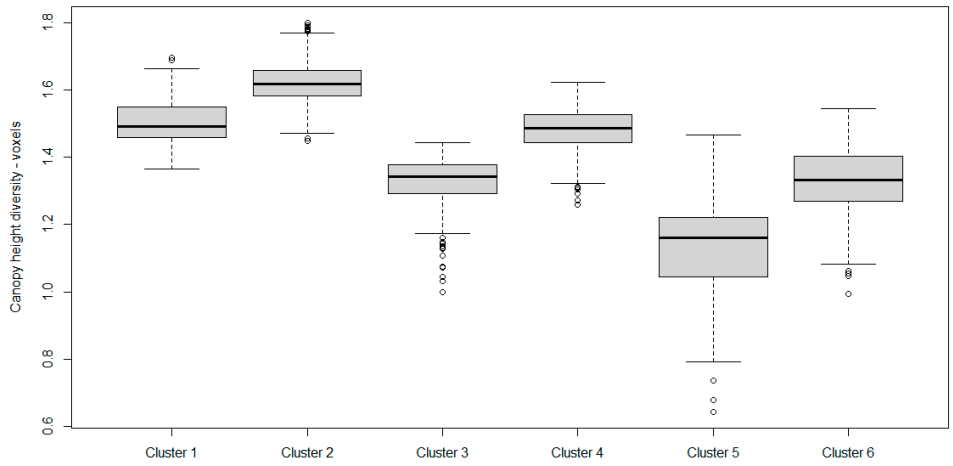

Figure 7. Boxplots for the CHD_V by individual clusters of stand types.

Table 2. Area, dominant height, canopy closure, and canopy height diversity using voxels (CHD_V) by individual clusters of stand types.

Cluster	Area (ha)	H_{dom} (m)	SD_1	CV_1 (%)	Canopy Closure	SD_2	CV_2 (%)	CHD_V	SD_3	CV_3 (%)
1	569.3	26.4	2.9	11.0	0.84	0.06	7.2	1.50	0.06	4.1
2	968.9	36.8	2.9	7.9	0.95	0.04	3.8	1.62	0.06	3.6
3	941.1	25.4	3.0	11.9	0.91	0.05	5.4	1.33	0.07	5.2
4	1533.9	32.2	2.7	8.5	0.95	0.03	3.6	1.48	0.06	4.1
5	157.2	13.1	3.2	24.4	0.41	0.13	31.2	1.12	0.15	13.4
6	309.1	19.2	2.7	14.0	0.69	0.09	13.6	1.33	0.10	7.4

The results of the first analysis using the CHM revealed that nearly 50% of the entire investigated area belonged to uneven-aged forests, namely Clusters 2 and 4 (Table 3, Figure 8), with a forest area of 4479 ha. In the second analysis, Cluster 3 was classified as mature even-aged forests, and after a detailed visual inspection, Cluster 4, with a slightly higher average canopy height diversity determined from voxels, was also classified as mature even-aged forests.

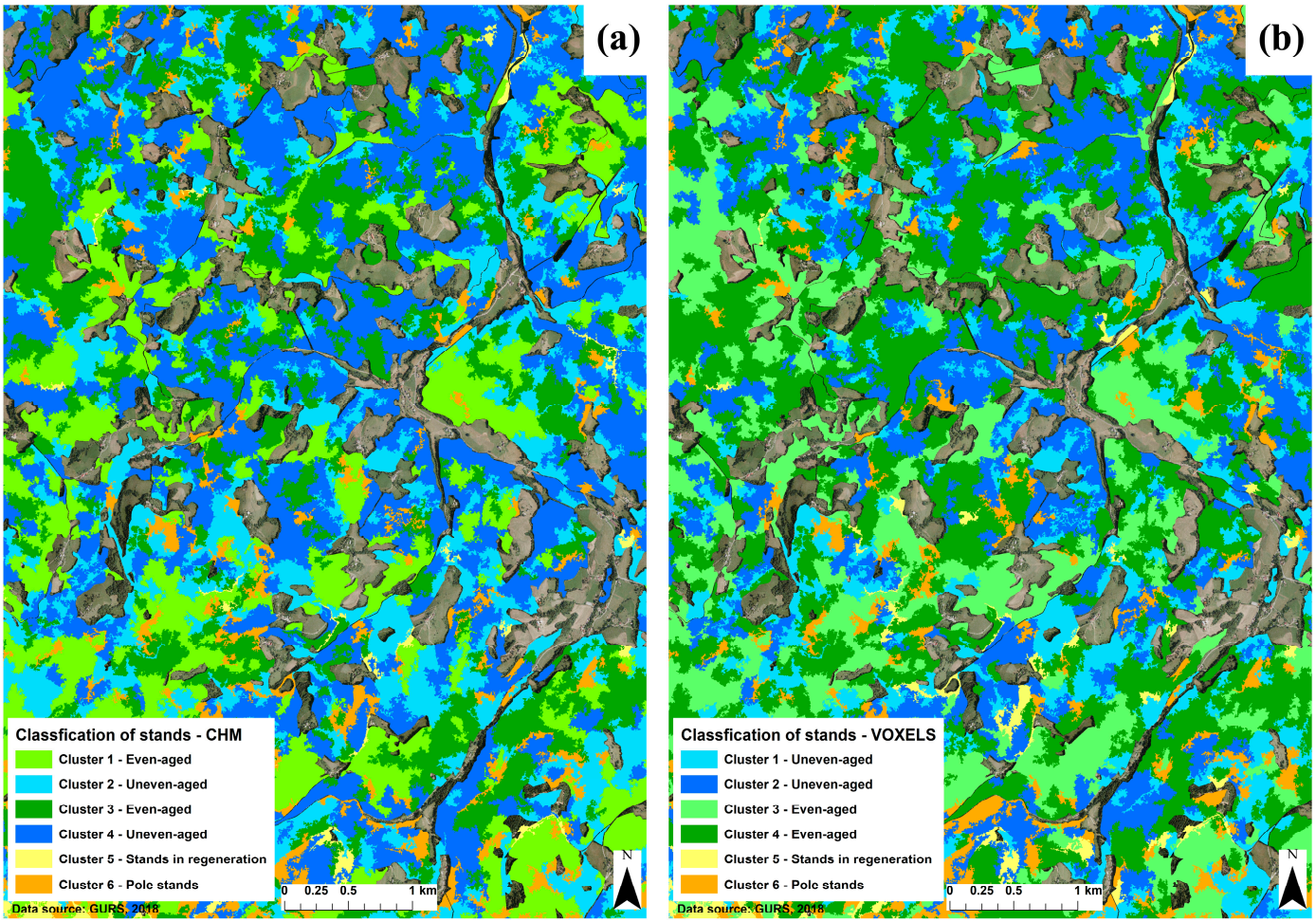

Figure 8. Map of classified stands. CHM (**a**) and voxels (**b**) were used to assess the canopy height diversity.

Table 3. Area proportions of stand structures for the assessment of canopy height diversity using the CHM and voxels.

CHM \ VOXELS	Cluster 1	Cluster 2	Cluster 3	Cluster 4	Cluster 5	Cluster 6	Total
Cluster 1	1.1	0.0	14.6	5.9	0.0	0.0	21.6
Cluster 2	10.7	0.0	4.1	2.0	0.0	1.4	18.2
Cluster 3	0.0	6.6	1.2	11.7	0.0	0.0	19.5
Cluster 4	0.6	15.0	0.9	14.6	0.0	0.0	31.1
Cluster 5	0.0	0.0	0.0	0.0	2.6	0.2	2.8
Cluster 6	0.3	0.0	0.2	0.0	0.9	5.4	6.8
Total	12.7	21.6	21.0	34.2	3.5	7.0	100.0

3.2. Validation of the Classification of Permanent Sample Plots

By comparing the permanent sample plots using the systematic grid, we investigated whether there were statistically significant differences between the variables of the different stand types and examined the differences between even- and uneven-aged mature forest structures (Figure 9). When analyzing the height diversity with the CHM, mature, even-aged plots were classified as belonging to Clusters 1 and 3, and uneven-aged plots were attributed to Clusters 2 and 4. Considering the height diversity analysis with voxels, mature, even-aged plots were observed in Clusters 3 and 4, and uneven-aged plots were located in Clusters 1 and 2. Using CHM lidar, cross-sections of the lidar point cloud, and orthophoto, at least 20 individual stands of each cluster underwent visual inspection to validate the classification of even- and uneven-aged stands.

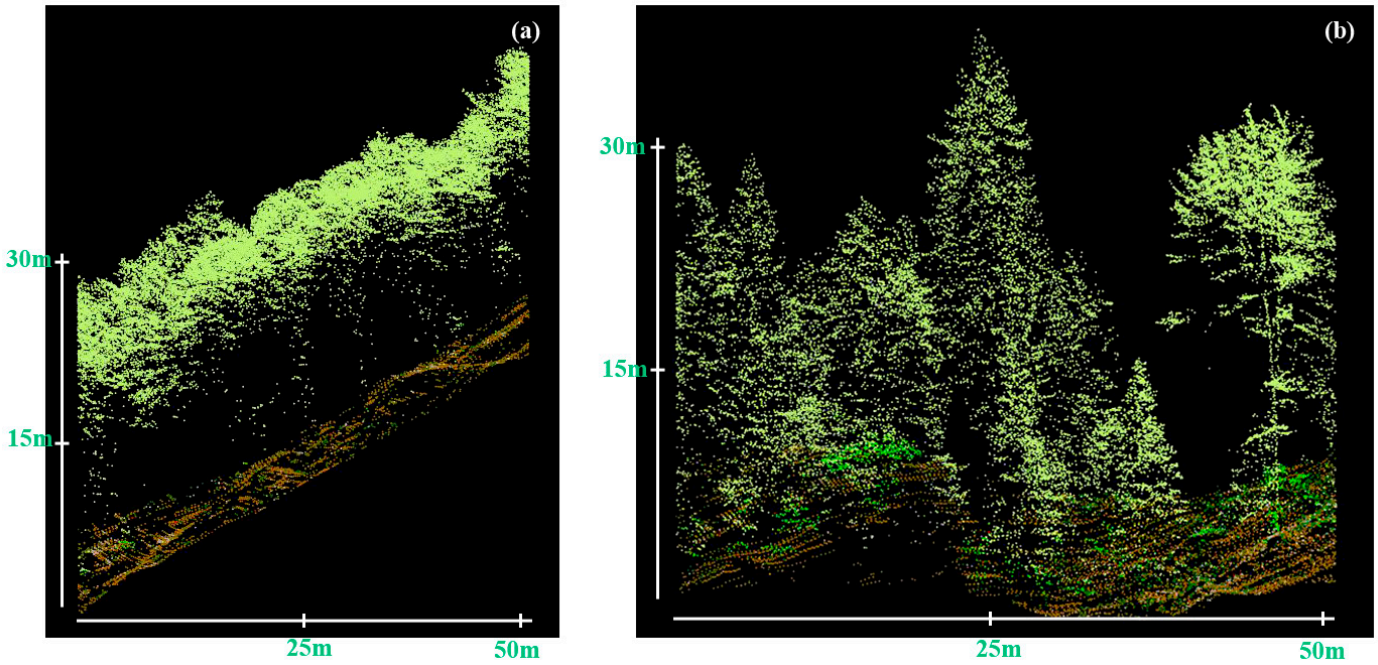

Figure 9. Examples of the cross-sections using the lidar point cloud data of an even-aged stand (**a**) and uneven-aged stand (**b**).

Regarding the assessment of canopy height diversity, with both methods, uneven-aged stands had a higher dominant height, which was statistically significant ($p < 0.05$; *t*-test and $p < 0.001$; *t*-test) (Figure 10a). The homogeneity index was statistically significantly higher in the first analysis (CHM) ($p < 0.05$; *t*-test) and marginally statistically significant in the second analysis ($p < 0.01$; Wilcoxon rank-sum test). The Shannon's diversity index (basal area) was higher in heterogeneous stand structures but not statistically significant. The

basal area was larger in the first analysis and slightly smaller in the second analysis, but the differences in mean values were not statistically significant (Figure 10b).

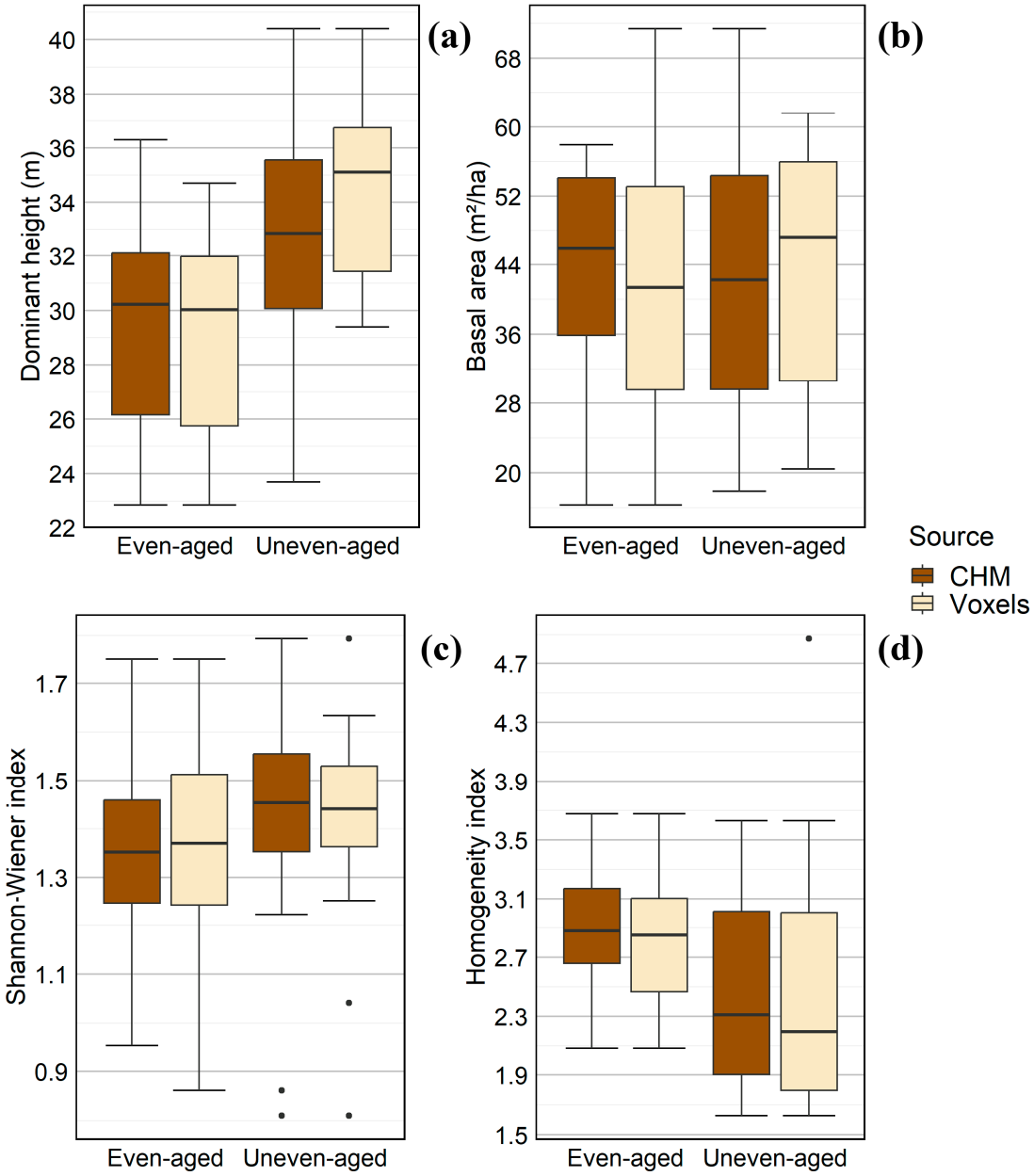

Figure 10. Boxplots for the variables dominant height (**a**), basal area (**b**), Shannon's diversity index (basal area) (**c**), and De Camino homogeneity index (**d**) for mature even- and uneven-aged forest stands in the study area of the Pahernik estate using the CHM and voxels to estimate canopy height diversity (first and second analysis).

4. Discussion

The classification of forest structures across spatiotemporal scales is important for forest monitoring and management [53], especially in the context of climate change and recent events in temperate forests [54,55]. Given the changes in site conditions, the increasing frequency of disasters, and the threat to forests from harmful organisms, Diaci et al. [56] have highlighted the optimization of silvicultural measures in even- and uneven-aged forests as one of the development priorities in this field. The planning and optimization of these measures will be significantly more successful in uneven-aged forests if we know the

locations and types of stand structures using remote sensing data of vertical structures. It is precisely these forms of stand structure that are characteristic of the Pahernik estate and its surroundings, which involve a freestyle technique of silviculture with the implementation of different silvicultural systems in small areas of the same segment [57].

In this study, we identified uneven-aged forests with spruce as the predominant tree species (more than 60% of the growing stock) at the stand level (polygon), not at the raster cell or sample plot level, as in most previous studies [53,58]. When analyzing the lidar data, we used the dominant height, canopy closure, and canopy height diversity. The dominant height derived from lidar data was also used by Bončina, Trifković, and Rosset [22] for stand classification in even- and uneven-aged structures, as well as the cover levels in stand layers. Torresan et al. [59] categorized forests with similar tree composition into pole-stage, young, adult, mature, and old forests using 18 variables derived from lidar data. In another study, Torresan, et al. [60] predicted forest structure classes from lidar CHM data, highlighting the need for professionals involved in forest management planning to familiarize themselves with CHM approach [60].

The main advantage of the selected classification variables used in the present study is that they are also easy to use in operational forestry. In operational practice, diversity data are often lost when delineating forest stands, as diverse stands are often classified as, e.g., mature stands. Therefore, we sought to present a simple method for classifying uneven-aged forests into homogeneous stand types that preserve data on their diversity. In uneven-aged forests, all developmental stages are found in a very small area, and regeneration phases are not specifically recorded [61]. Freely available lidar data [24] with a low number of pulses recorded nationwide were used for the current survey. The lidar data were recorded in 2014, and the field measurements were carried out in 2013. We assume that the minimal temporal difference between the field measurement and the lidar recording time had no significant impact on the validation of the lidar data with the field measurements. We explain this with the low intensity of small-scale forest management in the study area in small gaps [27] and the fact that the height growth of Norway spruce, the dominant tree species in this area, is between 28 and 40 cm per year at a similar site [62].

The proposed methodology can be further applied using permanent sample plots' data from national forest inventories of most European nations, as lidar data are freely available in these countries [36]. A limitation of the study is the potential loss of forest structure detail (especially in the voxel approach) due to the use of low resolution lidar data. However, the advantage is the free availability of these data and their accessibility for the whole country and thus the possibility of further studies in other Slovenian forests with different tree species compositions and structures.

The application of the proposed approach is also suitable for other temperate forests and for forests in other climatic zones, but the height classes (in our case 5 m) for estimating canopy height diversity and canopy cover as well as the radius (in our case 3 m) for detecting tree tops from lidar data need to be adapted to the conditions in these forests. Caution is advised when using this approach in forests with steep slopes, as the accuracy of tree height and canopy height diversity detection from lidar data decreases [63]. The presented classification of forest stand structure should be continued in future studies using higher resolution lidar data and by complementing the classification with tree species mixtures or tree composition based on airborne hyperspectral data [64].

To determine the diversity of forest structures, we developed a canopy height model from lidar data because it is simple and suitable for use in various imaging segmentation methods [65], and voxels were used because this analysis method has significant potential to improve the accuracy of forest measurements [42] or stand characteristics. Both methods yielded the same results considering even- and uneven-aged stands, although the differences in vertical diversity between even- and uneven-aged stands were greater when using the CHM. We conclude that in areas with low laser scanner density, CHM analysis is a more appropriate method for assessing forest stand heterogeneity. At higher laser densities than those indicated by Pearse, Watt, Dash, Stone, and Caccamo [42], the use of voxels is recom-

mended, due to the ability to detect shade-tolerant trees under a dense canopy of mature dominant trees. In our study area, stand regeneration is concentrated in small gaps [27], so we believe that trees identified as the understory according to CHD_{CHM} classification did not have a significant effect, which was confirmed by the larger SD in the dominant height of uneven-aged stands (Figure 6). The resilience of stands to natural disturbances is mainly influenced by the height heterogeneity of trees in the canopy [66], which was found to be adequate based on the CHD_{CHM} classification. For multilayered stands, which do not occur in the study area in practice, a greater influence of height heterogeneity on the stand classification with CHD_{CHM} is expected. However, the lower-than-expected results of the voxel classification are mainly due to the low density of laser scanning. By using voxels, which are metrics that provide better descriptions of complex forest structures [67], we have thus demonstrated the potential of understory detection for stand classification, which will become increasingly significant in the future as the density of national lidar surveys is likely to increase. Similar to Hamraz, et al. [68], we also found a higher detection accuracy of understory trees at higher laser scanning densities.

In both validation analyses with data from permanent plots (Figure 10), the dominant height was statistically significantly higher in uneven-aged forests, which was also demonstrated by Sterba and Ledermann [69]. The basal area had the same size in even-aged and uneven-aged stands. The homogeneity index was statistically significantly lower in uneven-aged forests. Similar values of this index were also found in uneven-aged spruce, fir, and beech forests by Ibrahimspahić, Balić, and Lojo [50]. The Shannon–Wiener index, calculated from the basal area of the trees in the plots, was higher in uneven-aged forests, but the difference was not statistically significant, which is due to the different diameters at breast height of the trees with the same dominant stand height. These findings validate the classification of stands based on lidar data into even- and uneven-aged structures. The higher, but not statistically significant, Shannon–Wiener index in the first classification using CHD_{CHM} can be attributed to the inability to detect trees in the understory using this approach, as well as the low density of laser scanning in the CHM_V analysis. However, the validity of both approaches was confirmed by the statistically significantly different heterogeneity index values. In the CHD_{CHM} analysis, a higher standard deviation in the dominant tree height within stands was observed in uneven-aged stands (Figure 6).

5. Conclusions

The resilience of uneven-aged forest stands to disturbances, calamities, and climate change makes their development and identification crucial. The use of freely available nationwide lidar data to identify uneven-aged forest stands offers a cost-effective, efficient, and objective alternative to traditional field measurements.

In areas with low laser scanning density, CHM analysis is a more appropriate method for assessing forest stand height heterogeneity. The advantage of detecting uneven-aged structures using voxels is the ability to detect shade-tolerant species of varying age classes beneath a dense canopy of mature, dominant trees. Therefore, in areas where higher-density laser scanning data are available, using voxels is recommended for assessing the heterogeneity of forest stand heights and classifying stands into even- and uneven-aged types.

Author Contributions: Conceptualization, A.M.P. and M.S.; methodology, A.M.P. and M.S.; software, A.M.P. and M.S.; validation, A.M.P. and M.S.; formal analysis, A.M.P. and M.S.; investigation, A.M.P. and M.S.; resources, A.M.P. and M.S.; data curation, A.M.P. and M.S.; writing—original draft preparation, A.M.P. and M.S.; writing—review and editing, A.M.P. and M.S.; visualization, A.M.P. and M.S.; supervision, M.S.; project administration, A.M.P. and M.S.; funding acquisition, A.M.P. and M.S. All authors have read and agreed to the published version of the manuscript.

Funding: The work was produced as a section of the studies of the first author's doctoral study program in Biosciences, funded by the Ministry of Education, Science and Sport of the Republic of Slovenia and the Pahernik Foundation, and as part of the Research Programme P4-0107 Forest Biology, Ecology and Technology and the Development funding pillar of the Slovenian Forestry

Institute and the research project J2-3055 ROVI—Innovative radar and optical satellite image time series fusion and processing for monitoring the natural environment were funded by the Slovenian Research and Innovation Agency and the project Obtaining information on changes in carbon stocks in living and dead biomass in forests, founded by Ministry of Agriculture, Forestry and Food of the Republic of Slovenia and Ministry of the Environment and Spatial Planning of the Republic of Slovenia.

Data Availability Statement: The authors confirm that the data underlying this research are included in the article. The raw data that support the results are available upon reasonable request from the corresponding author.

Acknowledgments: We would like to thank Andrej Grah for his help in preparing the figures. We are also grateful to Andrej Kobler for creating the canopy height model and the voxels from the data of the Laser Scanning of Slovenia and David Hladnik for his advice in the initial phase of developing the methodology. We greatly appreciate the valuable suggestions for improvement made by all reviewers.

Conflicts of Interest: The authors declare no conflicts of interest. The funders had no role in the design of the study; in the collection, analyses, or interpretation of data; in the writing of the manuscript; or in the decision to publish the results.

References

1. Kuuluvainen, T.; Tahvonen, O.; Aakala, T. Even-Aged and Uneven-Aged Forest Management in Boreal Fennoscandia: A Review. *Ambio* **2012**, *41*, 720–737. [CrossRef] [PubMed]
2. Kukunda, C.B.; Beckschäfer, P.; Magdon, P.; Schall, P.; Wirth, C.; Kleinn, C. Scale-guided mapping of forest stand structural heterogeneity from airborne LiDAR. *Ecol. Indic.* **2019**, *102*, 410–425. [CrossRef]
3. Spiecker, H. Silvicultural management in maintaining biodiversity and resistance of forests in Europe—Temperate zone. *J. Environ. Manag.* **2003**, *67*, 55–65. [CrossRef] [PubMed]
4. Zeller, L.; Liang, J.; Pretzsch, H. Tree species richness enhances stand productivity while stand structure can have opposite effects, based on forest inventory data from Germany and the United States of America. *For. Ecosyst.* **2018**, *5*, 4. [CrossRef]
5. Forrester, D.I. Linking forest growth with stand structure: Tree size inequality, tree growth or resource partitioning and the asymmetry of competition. *For. Ecol. Manag.* **2019**, *447*, 139–157. [CrossRef]
6. Schütz, J.-P.; Saniga, M.; Diaci, J.; Vrška, T. Comparing close-to-nature silviculture with processes in pristine forests: Lessons from Central Europe. *Ann. For. Sci.* **2016**, *73*, 911–921. [CrossRef]
7. ForestEurope. *State of Europe's Forests 2015 Report*; Ministerial Conference on the Protection of Forests in Europe, FOREST EUROPE Liaison Unit Madrid: Madrid, Spain, 2015; p. 312.
8. Lafond, V.; Lagarrigues, G.; Cordonnier, T.; Courbaud, B. Uneven-aged management options to promote forest resilience for climate change adaptation: Effects of group selection and harvesting intensity. *Ann. For. Sci.* **2014**, *71*, 173–186. [CrossRef]
9. Diaci, J.; Roženbergar, D.; Fidej, G.; Nagel, T.A. Challenges for Uneven-Aged Silviculture in Restoration of Post-Disturbance Forests in Central Europe: A Synthesis. *Forests* **2017**, *8*, 378. [CrossRef]
10. Dănescu, A.; Albrecht, A.T.; Bauhus, J.; Kohnle, U. Geocentric alternatives to site index for modeling tree increment in uneven-aged mixed stands. *For. Ecol. Manag.* **2017**, *392*, 1–12. [CrossRef]
11. Bončina, A.; Diaci, J.; Cenčič, L. Comparison of the two main types of selection forests in Slovenia: Distribution, site conditions, stand structure, regeneration and management. *For. Int. J. For. Res.* **2002**, *75*, 365–373. [CrossRef]
12. ReNGP. Resolucija o Nacionalnem Gozdnem Programu (Uradni list RS (Official Gazette of the Republic of Slovenia), No. 111/07). 2007. Available online: https://www.uradni-list.si/glasilo-uradni-list-rs/vsebina/2007-01-5510 (accessed on 9 July 2024).
13. Klopčič, M.; Bončina, A. Recruitment of tree species in mixed selection and irregular shelterwood forest stands. *Ann. For. Sci.* **2012**, *69*, 915–925. [CrossRef]
14. Trifković, V.; Bončina, A.; Ficko, A. Recruitment of European beech, Norway spruce and silver fir in uneven-aged forests: Optimal and critical stand, site and climatic conditions. *For. Ecol. Manag.* **2023**, *529*, 120679. [CrossRef]
15. Trifković, V.; Bončina, A.; Ficko, A. Density-dependent mortality models for mono- and multi-species uneven-aged stands: The role of species mixture. *For. Ecol. Manag.* **2023**, *545*, 121260. [CrossRef]
16. Maltamo, M.; Packalén, P.; Yu, X.; Eerikäinen, K.; Hyyppä, J.; Pitkänen, J. Identifying and quantifying structural characteristics of heterogeneous boreal forests using laser scanner data. *For. Ecol. Manag.* **2005**, *216*, 41–50. [CrossRef]
17. Nowak, D.J.; Crane, D.E.; Stevens, J.C.; Hoehn, R.E.; Walton, J.T.; Bond, J. A ground-based method of assessing urban forest structure and ecosystem services. *Aboriculture Urban For.* **2008**, *34*, 347–358. [CrossRef]
18. Coops, N.C.; Hilker, T.; Wulder, M.A.; St-Onge, B.; Newnham, G.; Siggins, A.; Trofymow, J.A. Estimating canopy structure of Douglas-fir forest stands from discrete-return LiDAR. *Trees* **2007**, *21*, 295. [CrossRef]
19. Hladnik, D.; Žižek Kulovec, L. Consistency of stand density estimates and their variability in forest inventories in Slovenia. *Acta Silvae Et Ligni* **2014**, *104*, 1–14. [CrossRef]

20. Zimble, D.A.; Evans, D.L.; Carlson, G.C.; Parker, R.C.; Grado, S.C.; Gerard, P.D. Characterizing vertical forest structure using small-footprint airborne LiDAR. *Remote Sens. Environ.* **2003**, *87*, 171–182. [CrossRef]
21. Hall, S.A.; Burke, I.C.; Box, D.O.; Kaufmann, M.R.; Stoker, J.M. Estimating stand structure using discrete-return lidar: An example from low density, fire prone ponderosa pine forests. *For. Ecol. Manag.* **2005**, *208*, 189–209. [CrossRef]
22. Bončina, A.; Trifković, V.; Rosset, C. Forest stand segmentation using lidar data. *Gozdarski Vestn.* **2024**, *82*, 24–34.
23. Lim, K.; Treitz, P.; Wulder, M.; St-Onge, B.; Flood, M. LiDAR remote sensing of forest structure. *Prog. Phys. Geogr. Earth Environ.* **2003**, *27*, 88–106. [CrossRef]
24. GURS. *Data from the Laser Scanning of Slovenia Project*; MNRSP—Surveying and Mapping Authority of the Republic of Slovenia: Ljubljana, Slovenia, 2015.
25. Sušek, M. *Pahernikovi gozdovi: Biografija rodbine Pahernik*; Pahernikov sklad: Radlje, Slovenia, 2005; p. 83.
26. Pintar, A.M.; Hladnik, D. Strukturna pestrost gozdnih sestojev na Pahernikovi gozdni posesti. *Acta Silvae Ligni* **2018**, *117*, 1–16. [CrossRef]
27. Pintar, A.M.; Skudnik, M. Usefulness of National Airborne Laser Scanning and Aerial Survey Data in Forest Canopy Gap Detection. *Geod. Vestn.* **2024**, *68*, 180–193. [CrossRef]
28. ZGS. *Posestni Načrt za Gozdove Pahernikove Ustanove 2014–2023*; Slovenia Forest Service: Slovenj Gradec, Slovenia, 2015; p. 90.
29. MKGP. *Grafični Podatki RABA za Celo Slovenijo*; Ministry of Agriculture, Forestry, and Food: Ljubljana, Slovenia, 2015.
30. Pegan Žvokelj, B.; Bric, V.; Triglav Čekada, M.; Obreza, A.; Tršan, S.; Dejak, B.; Karničnik, I. *Izvedba lasreskega skeniranja Slovenije: Blok 23: Tehnično Poročilo o Izdelavi Izdelkov*; Geodetski inštitut Slovenije: Ljubljana, Slovenia, 2015; p. 19.
31. Kobler, A. *Canopy Height Model Derived from the Laser Scanning of Slovenia*; Slovenian Forestry Institute: Ljubljana, Slovenia, 2015.
32. Šprah, R. *Ocenjevanje Ekotipov v Gozdnogospodarski Enoti Lovrenc na Pohorju*; Biotehniška fakulteta, Oddelek za gozdarstvo in obnovljive gozdne vire: Ljubljana, Slovenia, 2019.
33. Pretzsch, H.; Biber, P.; Uhl, E.; Dahlhausen, J.; Rötzer, T.; Caldentey, J.; Koike, T.; van Con, T.; Chavanne, A.; Seifert, T.; et al. Crown size and growing space requirement of common tree species in urban centres, parks, and forests. *Urban For. Urban Green.* **2015**, *14*, 466–479. [CrossRef]
34. Tarmu, T.; Laarmann, D.; Kiviste, A. Mean height or dominant height—What to prefer for modelling the site index of Estonian forests? *For. Stud.* **2020**, *72*, 121–138. [CrossRef]
35. FAO. *Global Forest Resources Assessment, 2020; Guidelines and Specifications FRA 2020*; FAO: Rome, Italy, 2020.
36. Hladnik, D.; Kobler, A.; Pirnat, J. Evaluation of Forest Edge Structure and Stability in Peri-Urban Forests. *Forests* **2020**, *11*, 338. [CrossRef]
37. Stark, S.C.; Leitold, V.; Wu, J.L.; Hunter, M.O.; de Castilho, C.V.; Costa, F.R.C.; McMahon, S.M.; Parker, G.G.; Shimabukuro, M.T.; Lefsky, M.A.; et al. Amazon forest carbon dynamics predicted by profiles of canopy leaf area and light environment. *Ecol. Lett.* **2012**, *15*, 1406–1414. [CrossRef] [PubMed]
38. Palace, M.W.; Sullivan, F.B.; Ducey, M.J.; Treuhaft, R.N.; Herrick, C.; Shimbo, J.Z.; Mota-E-Silva, J. Estimating forest structure in a tropical forest using field measurements, a synthetic model and discrete return lidar data. *Remote Sens. Environ.* **2015**, *161*, 1–11. [CrossRef]
39. Hirschmugl, M.; Lippl, F.; Sobe, C. Assessing the Vertical Structure of Forests Using Airborne and Spaceborne LiDAR Data in the Austrian Alps. *Remote Sens.* **2023**, *15*, 664. [CrossRef]
40. Kobler, A. *Voxels from the Laser Scanning of Slovenia, Slovenian Forestry Institute*; Slovenian Forestry Institute: Ljubljana, Slovenia, 2020.
41. Fassnacht, F.E.; Mager, C.; Waser, L.T.; Kanjir, U.; Schäfer, J.; Buhvald, A.P.; Shafeian, E.; Schiefer, F.; Stančič, L.; Immitzer, M.; et al. Forest practitioners' requirements for remote sensing-based canopy height, wood-volume, tree species, and disturbance products. *For. Int. J. For. Res.* **2024**, *cpae021*, 1–20. [CrossRef]
42. Pearse, G.D.; Watt, M.S.; Dash, J.P.; Stone, C.; Caccamo, G. Comparison of models describing forest inventory attributes using standard and voxel-based lidar predictors across a range of pulse densities. *Int. J. Appl. Earth Obs. Geoinf.* **2019**, *78*, 341–351. [CrossRef]
43. Jacon, A.D.; Galvão, L.S.; Martins-Neto, R.P.; Crespo-Peremarch, P.; Aragão, L.E.O.C.; Ometto, J.P.; Anderson, L.O.; Vedovato, L.B.; Silva-Junior, C.H.L.; Lopes, A.P.; et al. Characterizing Canopy Structure Variability in Amazonian Secondary Successions with Full-Waveform Airborne LiDAR. *Remote Sens.* **2024**, *16*, 2085. [CrossRef]
44. Liu, X.; Ma, Q.; Wu, X.; Hu, T.; Liu, Z.; Liu, L.; Guo, Q.; Su, Y. A novel entropy-based method to quantify forest canopy structural complexity from multiplatform lidar point clouds. *Remote Sens. Environ.* **2022**, *282*, 113280. [CrossRef]
45. Ming, L.; Liu, J.; Quan, Y.; Li, M.; Wang, B.; Wei, G. Mapping tree species diversity in a typical natural secondary forest by combining multispectral and LiDAR data. *Ecol. Indic.* **2024**, *159*, 111711. [CrossRef]
46. UC. K-Means Cluster Analysis. UC Business Analytics R Programming Guide. 2020. Available online: https://uc-r-github.io/kmeans_clustering (accessed on 23 April 2020).
47. Stepper, C.; Straub, C.; Pretzsch, H. Assessing height changes in a highly structured forest using regularly acquired aerial image data. *For. Int. J. For. Res.* **2014**, *88*, 304–316. [CrossRef]
48. SFS. Slovenia Forest Service. 2024. Available online: http://www.zgs.si/eng/homepage/index.html (accessed on 10 July 2024).
49. de Camino, R. Determinación de la Homogeneidad de Rodales. *Bosque* **1976**, *1*, 110–115. [CrossRef]

50. Ibrahimspahić, A.; Balić, L.; Lojo, A. Homogeneity of fir and spruce forest stands in the manegement unit "Igman". In Proceedings of the International Sceientific Confrerence, Forest in the Future—Sustainable Use, Risks and Challanges, Belgrade, Serbia, 4–5 October2012; pp. 115–121.
51. ESRI. *ArcMap*, version 10.8; ESRI: Redlands, CA, USA, 2018.
52. R_Core_Team. R: A Language and Environment for Statistical Computing; R Foundation Statistical Computing. 2020. Available online: http://www.R-project.org (accessed on 23 April 2020).
53. Tijerín-Triviño, J.; Moreno-Fernández, D.; Zavala, M.A.; Astigarraga, J.; García, M. Identifying Forest Structural Types along an Aridity Gradient in Peninsular Spain: Integrating Low-Density LiDAR, Forest Inventory, and Aridity Index. *Remote Sens.* **2022**, *14*, 235. [CrossRef]
54. Kutnar, L.; Kermavnar, J.; Pintar, A.M. Climate change and disturbances will shape future temperate forests in the transition zone between Central and SE Europe. *Ann. For. Res.* **2021**, *64*, 67–86. [CrossRef]
55. Kermavnar, J.; Kutnar, L.; Pintar, A.M. Ecological factors affecting the recent Picea abies decline in Slovenia: The importance of bedrock type and forest naturalness. *Iforest-Biogeosciences For.* **2023**, *16*, 105–115. [CrossRef]
56. Diaci, J.; Čater, M.; Grecs, Z.; Roženbergar, D.; Fidej, G.; Nagel, T.A. Raziskovalni in razvojni izzivi na področju gojenja gozdov. In Proceedings of the XXXIV. Gozdarski Študijski Dnevi, Ljubljana, Slovenia, 21–22 November 2017; p. 135.
57. Diaci, J. *Gojenje Gozdov: Pragozdovi, Sestoji, Zvrsti, Načrtovanje, Izbrana Poglavja*; University of Ljubljana, Biotechnical Faculty, Department of Forestry and Renewable Forest Resources: Ljubljana, Slovenia, 2006; p. 348.
58. Valbuena, R.; Maltamo, M.; Mehtätalo, L.; Packalen, P. Key structural features of Boreal forests may be detected directly using L-moments from airborne lidar data. *Remote Sens. Environ.* **2017**, *194*, 437–446. [CrossRef]
59. Torresan, C.; Corona, P.; Scrinzi, G.; Marsal, J.V. Using classification trees to predict forest structure types from LiDAR data. *Ann. For. Res.* **2016**, *59*, 281–298. [CrossRef]
60. Torresan, C.; Strunk, J.; Zald, H.S.J.; Zhiqiang, Y.; Cohen, W.B. Comparing statistical techniques to classify the structure of mountain forest stands using CHM-derived metrics in Trento province (Italy). *Eur. J. Remote Sens.* **2014**, *47*, 75–94. [CrossRef]
61. Veselič, Ž. Unsatisfactory Regeneration due to Overabundant Herbivorous Game is the Greatest Threat to the Conservation of Slovenian Forests. *Gozdarski Vesntik* **2017**, *75*, 383–397.
62. Kotar, M. *Zgradba, Rast in Donos Gozda na Ekoloških in Fizioloških Osnovah*; Zveza gozdarskih društev Slovenije in Zavod za gozdove Slovenije: Ljubljana, Slovenia, 2011; p. 500.
63. Tinkham, W.T.; Smith, A.M.S.; Hoffman, C.; Hudak, A.T.; Falkowski, M.J.; Swanson, M.E.; Gessler, P.E. Investigating the influence of LiDAR ground surface errors on the utility of derived forest inventories. *Can. J. For. Res.* **2012**, *42*, 413–422. [CrossRef]
64. Mäyrä, J.; Keski-Saari, S.; Kivinen, S.; Tanhuanpää, T.; Hurskainen, P.; Kullberg, P.; Poikolainen, L.; Viinikka, A.; Tuominen, S.; Kumpula, T.; et al. Tree species classification from airborne hyperspectral and LiDAR data using 3D convolutional neural networks. *Remote Sens. Environ.* **2021**, *256*, 112322. [CrossRef]
65. Kim, E.; Lee, W.-K.; Yoon, M.; Lee, J.-Y.; Son, Y.; Abu Salim, K. Estimation of Voxel-Based Above-Ground Biomass Using Airborne LiDAR Data in an Intact Tropical Rain Forest, Brunei. *Forests* **2016**, *7*, 259. [CrossRef]
66. Senf, C.; Mori, A.S.; Müller, J.; Seidl, R. The response of canopy height diversity to natural disturbances in two temperate forest landscapes. *Landsc. Ecol.* **2020**, *35*, 2101–2112. [CrossRef]
67. Whelan, A.W.; Cannon, J.B.; Bigelow, S.W.; Rutledge, B.T.; Sánchez Meador, A.J. Improving generalized models of forest structure in complex forest types using area- and voxel-based approaches from lidar. *Remote Sens. Environ.* **2023**, *284*, 113362. [CrossRef]
68. Hamraz, H.; Contreras, M.A.; Zhang, J. Forest understory trees can be segmented accurately within sufficiently dense airborne laser scanning point clouds. *Sci. Rep.* **2017**, *7*, 6770. [CrossRef]
69. Sterba, H.; Ledermann, T. Inventory and modelling for forests in transition from even-aged to uneven-aged management. *For. Ecol. Manag.* **2006**, *224*, 278–285. [CrossRef]